Vol. 26, No. 3

Complex Formation with Damage Recognition Protein Rad14 Is Essential for *Saccharomyces cerevisiae* Rad1-Rad10 Nuclease To Perform Its Function in Nucleotide Excision Repair In Vivo

Sami N. Guzder,[1] Christopher H. Sommers,[2] Louise Prakash,[1] and Satya Prakash[1]*

Sealy Center for Molecular Science, University of Texas Medical Branch, Galveston, Texas,[1] and Eastern Regional Research Center, USDA Agricultural Research Service, Wyndmoor, Pennsylvania[2]

Nucleotide excision repair (NER) in eukaryotes requires the assembly of a large number of protein factors at the lesion site which then coordinate the dual incision of the damaged DNA strand. However, the manner by which the different protein factors are assembled at the lesion site has remained unclear. Previously, we have shown that in the yeast *Saccharomyces cerevisiae*, NER proteins exist as components of different protein subassemblies: the Rad1-Rad10 nuclease, for example, forms a tight complex with the damage recognition protein Rad14, and the complex of Rad1-Rad10-Rad14 can be purified intact from yeast cells. As the Rad1-Rad10 nuclease shows no specificity for binding UV lesions in DNA, association with Rad14 could provide an effective means for the targeting of Rad1-Rad10 nuclease to damage sites in vivo. To test the validity of this idea, here we identify two *rad1* mutations that render yeast cells as UV sensitive as the *rad1Δ* mutation but which have no effect on the recombination function of Rad1. From our genetic and biochemical studies with these *rad1* mutations, we conclude that the ability of Rad1-Rad10 nuclease to associate in a complex with Rad14 is paramount for the targeting of this nuclease to lesion sites in vivo. We discuss the implications of these observations for the means by which the different NER proteins are assembled at the lesion site.

Nucleotide excision repair (NER) is a highly conserved repair system among eukaryotes. In the yeast *Saccharomyces cerevisiae*, a combination of Rad14, Rad4-Rad23, RPA, TFIIH, Rad1-Rad10, and Rad2 mediates the dual incision of the damaged DNA strand, releasing an ~30-nucleotide (nt) lesion-containing DNA fragment (6). Rad14, Rad4-Rad23, and RPA function at the damage recognition step. The Rad3 and Rad25 DNA helicases, which are the components of TFIIH, unwind the duplex DNA around the lesion, and the Rad1-Rad10 and Rad2 nucleases incise the damaged DNA strand on the 5′ and the 3′ side of the lesion, respectively (24). In humans, a combination of their respective counterparts, XPA, XPC-HR23B, RPA, TFIIH, XPF-ERCC1, and XPG, mediates the dual incision of the damaged DNA strand (19, 20). Similar to that in yeast, in humans, XPA, XPC-HR23B, and RPA act in damage recognition, the XPD and XPB helicases in TFIIH unwind the damaged duplex, and the XPF-ERCC1 and XPG nucleases incise the damaged strand on the 5′ and the 3′ side of the lesion, respectively (26, 27).

Previously, we have shown that the yeast NER proteins exist in vivo as components of separate protein subassemblies, named nucleotide excision repair factors (NEFs) 1 to 4. NEF1 is comprised of the damage recognition protein Rad14 and the Rad1-Rad10 nuclease, which incises the damaged strand on the 5′ side of the lesion (7). NEF2, the Rad4-Rad23 complex (6), is involved in damage recognition, and NEF3, comprised of TFIIH and the Rad2 endonuclease (12), promotes DNA

unwinding and 3′ incision (24). In yeast, the repair of the nontranscribed DNA strand and of transcriptionally inactive regions additionally requires the Rad7 and Rad16 proteins, which associate in a complex to form NEF4 (8); NEF4 binds preferentially to UV-damaged DNA in an ATP-dependent manner, and addition of NEF4 to the reconstituted system consisting of NEFs 1, 2, and 3 and RPA enhances the rate of incision of UV-damaged DNA (8).

Since neither the Rad1-Rad10 nuclease nor the Rad2 nuclease shows a specificity for binding the UV-damaged DNA (11, 30), we have suggested that the targeting of these nucleases to the damage sites in vivo is dependent upon their association with the other protein components of the respective NEF. Thus, association with Rad14 would be crucial for the targeting of the Rad1-Rad10 nuclease to DNA lesion sites (7), and association with TFIIH would promote the targeting of Rad2 nuclease to the lesion sites (12). Another model, however, posits that NER entails the sequential assembly of free NER factors at the lesion site; for example, from studies of in vivo distributions of NER proteins in human cells, it has been suggested that XPA and ERCC1-XPF arrive at the lesion site as separate entities rather than as part of the XPA-ERCC1-XPF ensemble, which is the human equivalent of yeast NEF1 (25).

In NEF1, Rad14 physically interacts with Rad1 and not with Rad10 (7). To test the validity of the idea that NER occurs by the sequential assembly of the NEFs at the lesion site and not via the sequential assembly of free NER factors, we have carried out genetic studies in yeast to determine if the physical association of Rad1 with Rad14 is a prerequisite for ensuring the targeting of the Rad1-Rad10 nuclease to the lesion sites in vivo. Since, in addition to its role in NER, the Rad1-Rad10 nuclease functions also in the single-strand annealing (SSA) pathway of genetic recombination (5, 15, 28, 29), and since

* Corresponding author. Mailing address: Sealy Center for Molecular Science, University of Texas Medical Branch at Galveston, 6.104 Blocker Medical Research Building, 11th and Mechanic Streets, Galveston, TX 77555-1061. Phone: (409) 747-8602. Fax: (409) 747-8608. E-mail: s.prakash@utmb.edu.

Rad1 is the catalytic subunit of the Rad1-Rad10 nuclease (1, 21) and is involved in direct physical interactions with Rad14 (7), we reasoned that it should be possible to isolate mutations of *RAD1* that inactivate only the NER function, resulting from defective interactions with the NER proteins, in particular, with the Rad14 protein, or which affect Rad1 interactions with the recombination proteins and thus confer only the recombination deficiency. Both the NER and recombination functions, however, would be affected if the mutation inactivates the nuclease function of Rad1 or disrupts the binding of Rad1 to Rad10 (2, 4).

   Here we report our studies with two *rad1* mutations which inactivate the NER function of the Rad1-Rad10 nuclease but have no effect upon its recombination function. Both the mutant Rad1 proteins associate with Rad10, and the protein complex displays a proficient nuclease activity. The mutant Rad1 proteins, however, have lost the ability to physically interact with Rad14. Interestingly, even though the mutant Rad1-Rad10 complex promotes proficient incision in the NER system reconstituted from purified proteins, these *rad1* mutations confer upon yeast cells the same high degree of UV sensitivity as does the *rad1Δ* mutation. This indicates that the two *rad1* mutations impose the same high degree of incision defect in vivo as that inflicted by the *rad1Δ* mutation. We discuss the implications of these observations and conclude that complex formation with Rad14 is essential for Rad1-Rad10 nuclease to perform its role in NER in vivo.

MATERIALS AND METHODS

Isolation of *rad1* mutations. The *RAD1* gene carried on the *URA3 CEN* plasmid pRR117 or pCS41 was mutagenized with hydroxylamine, which causes the deamination of cytosine to uracil and induces GC-to-AT transition mutations. The mutagenized plasmid was introduced into the *rad1Δ rad52Δ* strain RS69-8B (*MAT**a** arg4 trp5-27 ilv1-92 ura3-52 leu2-3,112 rad1Δ::URA3⁺ rad52Δ::TRP1⁺ HIS3::*pRS6), which also carries the *his3Δ3′ his3Δ5′* duplication. Transformants were plated and screened for sensitivity to UV light, and 250 UV-sensitive transformants were isolated. UV-sensitive transformants were then individually tested for their effect on recombination. Ten-milliliter cultures were grown to a density of 10^7 cells/ml in synthetic liquid medium which lacked both uracil and leucine. The uracil auxotrophy of RS69-8B was complemented by the *URA3* gene carried on pRR117 or pCS41. The *HIS3⁺* recombinants do not grow in medium lacking leucine due to the loss of the *LEU2* gene carried between the *his3* duplication (28, 29). Therefore, the frequency of *HIS3⁺* recombinants represents the actual recombination rate. Logarithmically growing cultures were collected by centrifugation, washed in sterile water, and plated on synthetic complete medium to determine viability and on synthetic complete medium lacking histidine to determine the frequency of *HIS3⁺* colonies.

   Since RS69-8B is a *rad1Δ rad52Δ* strain, UV-sensitive transformants that formed *HIS3⁺* recombinants at the rate observed in the *rad1Δ rad52Δ* strain were classified as deficient in both NER and recombination, while those which formed *HIS3⁺* recombinants at the rate observed in the *rad52Δ* strain were classified as recombination proficient. Two mutations which conferred UV sensitivity but were recombination proficient (Uvˢ Rec⁺) were identified among the 250 UV-sensitive transformants, and the plasmids carrying these *rad1* mutations were designated pCS5 and pCS126, respectively.

Mapping and sequence determination of *rad1* mutations. The *rad1* mutations responsible for the Uvˢ Rec⁺ phenotype and carried on plasmids pCS5 and pCS126, respectively, were mapped by complementation analysis, in which different DNA fragments from the mutant gene were replaced by the corresponding wild-type *RAD1* fragment. This analysis showed that both the *rad1* mutations mapped to a 602-bp EagI-BglII fragment present in the *RAD1* open reading frame from nucleotide positions +1746 to +2347, with the A of the initiating ATG being at position +1. DNA sequence analysis revealed that the *rad1* gene in plasmid pCS5 contained two G-to-A transitions, one in codon 750 and one in codon 752, resulting in a Glu-to-Lys and Ser-to-Asn change, respectively. By site-directed mutagenesis, we determined that the Uvˢ Rec⁺ phenotype of this

mutant results from the alteration of Glu750 to Lys, whereas the Ser752-to-Asn alteration has no effect. The *rad1* mutation in pCS126 contained a single G-to-A transition in codon 749, resulting in a Glu-to-Lys change.

Overproduction and purification of wild-type and mutant Rad1 proteins. The wild-type and mutant Rad1 proteins were expressed as glutathione *S*-transferase (GST) fusion proteins. The 3.3-kb BamHI fragment of *RAD1* was cloned into the BglII site of pBJ842 (13) to generate the *GAL:PGK:GST-RAD1* (2μm; *leu2-d*) plasmid pR1.47. A 1.7-kb BamHI-BglII fragment containing the K750 N752 and K749 *rad1* mutation, respectively, replaced the wild-type *RAD1* sequence in pR1.47 to give plasmids pR1.48 and pR1.49, respectively. The plasmids were checked by sequencing to reconfirm the identity of the *rad1* mutations. The yeast strain BJ5464, *MATα ura3-52 trp1 leu2Δ1 his3-Δ200 pep4::HIS3 prb1Δ1.6R can1 GAL* (obtained from the Berkeley Yeast Stock Center), carrying the plasmid pR1.47, pR1.48, or pR1.49 was treated with 1.5% galactose for ~7 h to induce the synthesis of the GST-Rad1 fusion proteins. Yeast cell paste was resuspended in cell breakage buffer (50 mM Tris-HCl, pH 7.5, 10% sucrose, 0.5 M NaCl, 1 mM EDTA) containing 2 mM dithiothreitol (DTT), 1 mM phenylmethylsulfonyl fluoride, and 10 μg/ml chymostatin, leupeptin, pepstatin, and aprotinin protease inhibitors. Yeast cells were lysed using the French press, and the crude lysate was clarified by centrifugation at $100,000 \times g$.

   The clarified lysate was passed over a glutathione-Sepharose 4B matrix (0.5 ml; Pharmacia) equilibrated in buffer A (50 mM Tris-HCl, pH 7.5, 0.5 mM EDTA, 1 mM DTT, 0.01% NP-40) containing 0.5 M NaCl. The column was washed sequentially with 10 volumes of buffer A containing 0.5 M, 1 M, and 0.15 M NaCl, and 50% (vol/vol) of the matrix was incubated with PreScission protease (2 μg/ml) to cleave the GST tag from the fusion protein. The Rad1 protein that appears in the supernatant was concentrated in a Centricon 30 and frozen at −70°C. The Sepharose matrix containing the bound GST-Rad1 fusion protein was used as an affinity matrix for interaction studies.

Interaction of Rad1 proteins with Rad14. Rad14 protein (10 pmol) was incubated for 4 h at 4°C with equimolar amounts of either wild-type Rad1 or mutant Rad1-K750 N752 or Rad1-K749 GST-fusion protein in complex with Rad10 and the complex bound to glutathione-Sepharose 4B. After removal of the supernatant containing the unbound Rad14 protein, the matrix was washed sequentially with buffer containing 0.1 M and 0.3 M NaCl. The Rad14 protein remaining bound was eluted with 2.0% sodium dodecyl sulfate (SDS) and visualized by immunoblot assay of a denaturing polyacrylamide gel.

DNA substrates for endonuclease assays. To generate the pseudo-Y DNA substrate, a 50-nt oligomer E (5′-CCCCCAAAAA GTCCACAGCC AGTCAA GTCA CCTTCTTGTC GTTCACCCTT-3′) radiolabeled at the 5′ end with T4 polynucleotide kinase and [γ-³²P]ATP (6,000 Ci/mmol; Amersham) was hybridized to a 50-nt oligomer A (5′-GGGACTGGAC TTGCCGACTT TGACTT GACT GGCTGTGGAC TTTTTGGGGG-3′). Annealing reactions were carried out by mixing 100 pmol of radiolabeled oligo E with 120 pmol unlabeled oligonucleotide A in 50 μl of buffer (50 mM Tris-Cl, pH 8.2, 10 mM MgCl₂, 0.2 mM EDTA, 1 mM DTT, and 0.1 mM spermidine) and incubating at 95°C for 2 min, at 65°C for 10 min, at 37°C for 20 min, and finally at 25°C for 30 min. The DNA substrate was purified by electrophoresis on a nondenaturing 7.5% polyacrylamide gel in Tris-borate-EDTA (TBE) buffer, and the DNA substrate was extracted from the gel by diffusion in Tris-EDTA buffer containing 50 mM NaCl overnight at 4°C.

   A similar protocol was followed to prepare the bubble DNA substrate using 5′-end-labeled 62-nt oligo G (5′-GACCTGCCCA ATTCTGGCTT GCACTG TGTG TGTGTGTGCG AGGTCTTTG CCCACGTTGA CCC-3′) annealed to oligo F (5′-GGGTCAACGT GGGCAAAGAC CTCGTTTTTT TTTTTTTTG TGCAAGCCAG AATTGGGCA GGTC-3′).

Endonuclease assays on pseudo-Y and bubble DNA substrates. Rad1-Rad10 protein complex (0.5 pmol) consisting of either the wild-type Rad1 protein or the mutant Rad1 protein was incubated with 0.1 pmol radiolabeled DNA substrate in reaction buffer (50 mM Tris-Cl, pH 7.5,1 mM DTT, 1 mM EDTA, 5 mM MgCl₂, 100 μg/ml bovine serum albumin) for 30 min at 30°C in a final reaction volume of 5 μl. The reaction was terminated by addition of 25 μl gel loading buffer (90% formamide in Tris-borate-EDTA buffer) and heating at 95°C for 3 min. The reaction products were resolved by running an aliquot on a 10% sequencing gel and autoradiography.

Incision of UV-damaged plasmid DNA. The NER proteins were individually purified from yeast cells harboring the overproducing plasmid for that particular protein, and TFIIH was purified from a wild-type yeast strain as described elsewhere (6). The incision reaction was carried out as described previously (6). Briefly, M13mp18 plasmid DNA (120 ng) unirradiated or irradiated with 254 nm UV (300 J/m²) was incubated with 60 ng RPA, 60 ng Rad4-Rad23 complex, 300 ng TFIIH, 30 ng Rad2, 30 ng Rad14, and 30 ng of either wild-type Rad1-Rad10 or mutant Rad1-K750 N752-Rad10, or Rad1-K749-Rad10 protein complex in
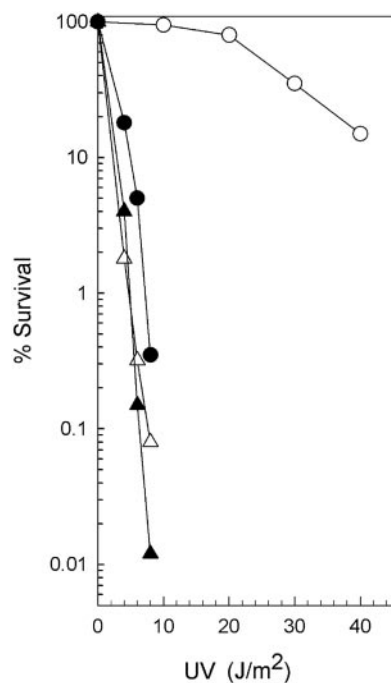
RESULTS

UV sensitivity and recombination proficiency of *rad1* mutations. We identified two *rad1* mutations that confer a high degree of UV sensitivity but are recombination proficient. One of these mutant *rad1* alleles harbored two alterations in which the Glu750 residue was changed to Lys and the Ser752 residue was changed to Asn. From the analyses of Lys750 and Asn752 mutations generated by site-directed mutagenesis, we determined that the Uv[s] Rec[+] phenotype of this *rad1* mutant allele results solely from the Glu750-to-Lys alteration. In the other mutant *rad1* allele, the Glu749 residue had been changed to Lys.

To quantitatively determine the effects of K750 N752 and K749 *rad1* mutations on NER, we introduced the plasmids pCS5 and pCS126, which carry these respective *rad1* mutations, into a *rad1*Δ strain and examined the UV sensitivity of the resulting strains. As is shown in Fig. 1, the *rad1*Δ strain harboring the plasmid pCS5 or pCS126 was as highly UV sensitive as the *rad1*Δ strain. The lack of any complementation of the UV sensitivity of the *rad1*Δ mutation by either of these *rad1* mutations indicates that similar to the *rad1*Δ mutation these *rad1* mutations lack the ability to incise UV-damaged DNA in vivo.

The effects of *rad1* mutations on genetic recombination were examined using the *his3*Δ3′ *his3*Δ5′ duplication, in which one copy of the *his3* gene is deleted at the 3′ end and the other is deleted at the 5′ end (28, 29). These two *his3* genes share homology of ~400 bp and are separated by the *LEU2* gene and pBR322 sequences. A functional *HIS3* gene is formed upon the loss of the intervening sequences between the two *his3* alleles, resulting from the recombination of two *his3* genes. Intrachromosomal mitotic recombination of this *his3* duplication is mediated by the Rad1-Rad10 nuclease (28, 29), which promotes recombination via SSA (5, 15), and also by genes of the *RAD52* group, which promote recombination via an alternate pathway (28, 29). As is shown in Table 1, the rate of *HIS3*^{+} recombinant formation was reduced by ~10-fold in the *rad1*Δ strain carrying the vector YCp50 compared to the *rad1*Δ

FIG. 1. UV sensitivity conferred by *rad1* mutations. Yeast *rad1*Δ strains carrying the vector YCp50 (△), the wild-type *RAD1* gene on plasmid pRR117 (○), the *rad1* mutation K750 N752 on plasmid pCS5 (▲), or the *rad1* mutation K749 on plasmid pCS126 (●) were grown to stationary phase at 30°C in synthetic complete medium lacking uracil. The cultures were diluted, plated, UV irradiated, and incubated in the dark at 30°C for 3 to 4 days. The colonies were counted, and survival was determined.

10 μl reaction buffer. After 30 min at 30°C, SDS and proteinase K were added to 0.5% and 200 μg/ml, respectively, followed by an additional incubation for 10 min at 37°C to deproteinize the reaction mixture. The samples were subjected to electrophoresis in a 0.8% agarose gel in Tris-acetate-EDTA buffer and stained with ethidium bromide to visualize the supercoiled and open circular DNA forms.

TABLE 1. Rate of *HIS3*^{+} recombinant formation in the wild-type strain and in *rad* mutant strains carrying the Uv[s] Rec[+] *rad1* mutation on plasmid pCS5 or pCS126

Genotype	Plasmid	Frequency of recombinants (per 10⁴ viable cells)			Mean frequency (±SD)	% of *RAD*[+] recombinants	% of *rad52*Δ recombinants
		Culture 1	Culture 2	Culture 3			
RAD[+]		2.08	4.13	6.48	4.35 ± 2.38		
*rad1*Δ	pRR117[a]	3.97	3.05	4.36	3.73 ± 0.68	100	
	pCS5	3.42	3.88	5.15	4.15 ± 0.89	111	
	pCS126	2.02	2.37	2.18	2.19 ± 0.18	58.7	
	YCp50	0.31	0.51	0.32	0.38 ± 0.11	10.2	
*rad52*Δ		0.42	0.25	0.21	0.29 ± 0.11		
*rad1*Δ *rad52*Δ[b]	pRR117	0.17	0.49	0.31	0.32 ± 0.16		100
	pCS5	0.11	0.20	0.16	0.16 ± 0.05		50
	pCS126	0.32	0.36	0.24	0.31 ± 0.06		96.2
	YCp50	0.008	0.007	0.04	0.02 ± 0.002		6.2
*rad1*Δ *rad52*Δ	pRR117	0.092	0.10	0.097	0.096 ± 0.003		100
	pCS5	0.08	0.072	0.083	0.079 ± 0.006		82.3
	pCS126	0.258	0.126	0.131	0.171 ± 0.007		178
	YCp50	0.013	0.006	0.007	0.008 ± 0.004		8.7

[a] YCp50 is the vector with no *RAD1* insert, pRR117 carries the wild-type *RAD1* gene, and pCS5 and pCS126 carry the K750 N752 and K749 *rad1* mutations, respectively.
[b] The two sets of entries for the *rad1*Δ *rad52*Δ strains represent data obtained from two different strains of the same genotype.

TABLE 2. Rate of *HIS3*⁺ recombinant formation in *cdc9* and in *cdc9 rad1*Δ carrying the *rad1* mutation on plasmid pCS5 or pCS126

Genotype	Plasmid	Frequency of recombinants (per 10^4 viable cells)			Mean frequency (±SD)
		Culture 1	Culture 2	Culture 3	
cdc9		147.9	99.2	203.8	150.3 ± 75.6
*cdc9 rad1*Δ	pRR117[a]	135.0	177.0	188.7	166.9 ± 45.1
	pCS5	138.8	173.4	124.5	145.6 ± 38.8
	pCS126	210.0	165.3	161.7	179.0 ± 27.2
	YCp50	16.2	31.9	11.5	19.8 ± 16.9

[a] YCp50 is the vector with no *RAD1* insert, pRR117 carries the wild-type *RAD1* gene, and pCS5 and pCS126 carry the K750 N752 and K749 *rad1* mutations, respectively.

strain harboring the wild-type *RAD1* gene carried on plasmid pRR117. Nearly wild-type levels of recombination proficiency were restored to the *rad1*Δ strain upon the introduction of either the *rad1* mutant plasmid pCS5 or pCS126.

A synergistic decline in the rate of *HIS3*⁺ recombination occurs in the *rad1*Δ *rad52*Δ double mutant compared to the rate in either single mutant (28, 29). Thus, while the recombination rate in the *rad1*Δ *rad52*Δ strain carrying the vector YCp50 declines by ~15-fold compared to the rate in the strain harboring the wild-type *RAD1* gene on plasmid pR117, introduction of either the plasmid pCS5 or pCS126 restored nearly the same level of recombination proficiency to the *rad1*Δ *rad52*Δ strain as that conferred by the wild-type *RAD1* gene (Table 1).

We also tested the effects of the two *rad1* mutations on *HIS3*⁺ recombinant formation in a *cdc9-ts* mutant strain defective in DNA ligase. At the restrictive temperature, *cdc9* exhibits a defect in the joining of Okazaki fragments (16). As a consequence of the increased half-life of unjoined Okazaki fragments, the *cdc9* mutant shows a hyper-recombinational phenotype, even at the permissive temperature (14, 18). The rate of *HIS3*⁺ recombination was examined at the permissive temperature (30°C) in the *cdc9* mutant and in the *cdc9 rad1*Δ mutant carrying the *his3*Δ3′ *his3*Δ5′ duplication. *HIS3*⁺ recombinants arise in the *cdc9* strain at a rate that is ~30- to 40-fold higher than that seen in the wild-type strain (compare the data in Tables 1 and 2). An ~8-fold reduction in recombination occurs in the *cdc9* mutant in the absence of *RAD1*, such as seen in the *cdc9 rad1*Δ strain carrying the YCp50 vector (Table 2). Introduction of the plasmid pCS5 or pCS126, which carries the *rad1* mutant gene, into the *cdc9 rad1*Δ strain restored the same level of hyper-recombinational proficiency to the strain as that conferred by the wild-type *RAD1* gene carried on plasmid pRR117 (Table 2). From all these observations, we conclude that neither the mutation K750 N752 nor the mutation K749 affects the recombination proficiency of *RAD1*.

Endonuclease activity of the Rad1-Rad10 complex is not affected by the UV-sensitive, recombination-proficient *rad1* mutations. The Rad1-Rad10 nuclease acts in a structure-specific manner, cleaving 3′-ended single-stranded DNA at its junction with duplex DNA (3). The DNA substrates that the Rad1-Rad10 nuclease would act upon during the SSA pathway of recombination versus those in NER, however, are expected to be quite different. In SSA, the Rad1-Rad10 nuclease would cleave the 3′-ended single-stranded DNA at its junction with

the duplex DNA, which would have resulted from the extensive 5′-to-3′ exonucleolytic degradation beginning at a double-stranded break, followed by the pairing of the homologous regions and the formation of nonhomologous 3′-ended tails (10). In NER, the Rad1-Rad10 nuclease would act upon the bubble DNA that would form at the lesion site from the combined action of the Rad3 and Rad25 DNA helicases in TFIIH (24). The NER defect of the *rad1* mutations might have arisen from the inability of the mutant Rad1-Rad10 protein complex to incise the bubble DNA substrate, and the recombination proficiency of these *rad1* mutations could then have resulted from their proficient ability for cleaving the 3′-ended single-stranded DNA at its junction with duplex DNA.

To examine the effects of *rad1* mutations on Rad1-Rad10 endonuclease activity, we used a pseudo-Y DNA substrate, which resembles the substrate that would be generated during the SSA recombination pathway, and a bubble DNA substrate which resembles the NER substrate. The purified Rad1-K750 N752 and Rad1-K749 mutant proteins (Fig. 2) were mixed with equimolar amounts of purified Rad10 and incubated overnight at 4°C to form the Rad1-Rad10 complex. The mutant or the wild-type Rad1-Rad10 complex was incubated with 5′-end-labeled pseudo-Y or bubble DNA substrate, and the reaction products were resolved on a sequencing gel and visualized by autoradiography. As is shown in Fig. 3, both the Rad1-K750 N752-Rad10 and Rad1-K749-Rad10 protein complexes could incise the pseudo-Y and bubble DNA substrates, and the pattern of incision products was the same as for the wild-type Rad1-Rad10 complex. From these observations, we conclude that the two *rad1* mutations do not significantly impair either the ability of Rad1 to associate with Rad10 or to perform
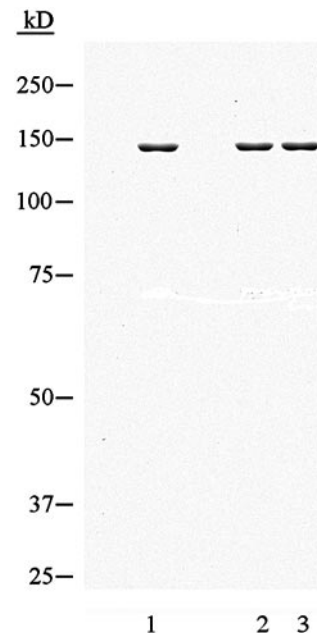

FIG. 2. Wild-type and mutant Rad1 proteins purified from yeast: wild-type protein (lane 1) or mutant Rad1 proteins K750 N752 and K749, respectively (lanes 2 and 3). A 0.5-μg aliquot of each protein was electrophoresed on a denaturing 7.5% polyacrylamide gel and stained with Coomassie brilliant blue.
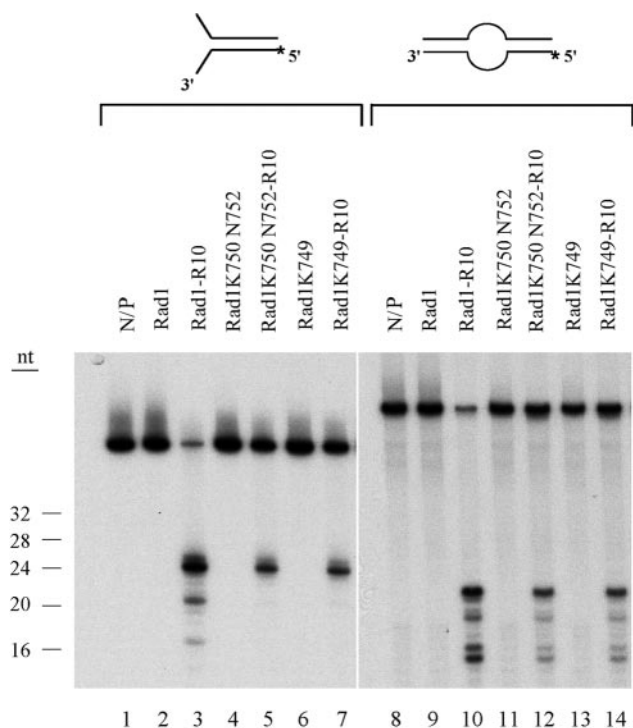
FIG. 3. Rad1 mutant proteins exhibit proficient endonuclease activity on pseudo-Y and bubble DNA substrates. A 5′-end-labeled pseudo-Y (lanes 1 to 7) or bubble (lanes 8 to 14) DNA substrate (0.1 pmol) was incubated without (lanes 1 and 8) or with 0.5 pmol of wild-type Rad1-Rad10 (lanes 3 and 10), Rad1-K750 N752-Rad10 (lanes 5 and 12), or Rad1-K749-Rad10 (lanes 7 and 14) for 30 min at 30°C. The wild-type Rad1 (lanes 2 and 9), Rad1-K750 N752 (lanes 4 and 11), and Rad1-K749 (lanes 6 and 13) proteins alone were also examined. The reaction products were analyzed on a 10% sequencing gel by autoradiography.

endonucleolytic scission on DNA intermediates that would be generated during NER or during recombination.

UV-sensitive recombination-proficient *rad1* mutations engender defective interactions with Rad14. The Rad1 and Rad10 proteins exist in vivo in a ternary complex with the damage recognition protein Rad14 (7). This protein assembly is very stable, as the three proteins copurify through Bio-Rex 70, DEAE Sephacel, hydroxyapatite, and Ni-nitrilotriacetic acid agarose, and they remain associated in the final Sephacryl 5-300 sizing column. In the Rad14-Rad1-Rad10 complex, Rad14 interacts directly with Rad1, and it interacts with the Rad1-Rad10 complex much more efficiently than with Rad1 alone.

To determine if the UV sensitivity of *rad1* mutations might have resulted from a defect in interaction with Rad14, we generated an affinity matrix wherein the GST–Rad1-Rad10 complex was bound to glutathione-Sepharose 4B matrix. Purified Rad14 was incubated with this affinity matrix, and the fraction of Rad14 remaining bound to the matrix after washing with increasing concentrations of NaCl was examined in the eluate following treatment with 2% SDS. The amounts of Rad14 protein in the supernatant, salt washes, and the SDS-eluate were then determined by electrophoresis on a 10% SDS-polyacrylamide gel and immunoblotting using affinity-purified Rad14 antibodies. As is shown in Fig. 4, in contrast to the wild-type Rad1-Rad10 complex, where Rad1 bound Rad14 very efficiently such that >90% of the input Rad14 protein remained bound to Rad1 (compare lanes 2 and 11), Rad14 did not bind either of the mutant Rad1 proteins (lanes 12 and 13) and >90% of Rad14 was found in the supernatant fraction (lanes 3 and 4).

Proficient incision of UV-damaged DNA in the reconstituted system by the mutant Rad1 proteins. Next, we examined the effects of the mutant Rad1 proteins in the reconstituted incision assay with UV-damaged plasmid DNA and purified NER proteins. In this assay, heterodimers of Rad1-K750 N752 and Rad1-K749 protein with the Rad10 protein were substituted
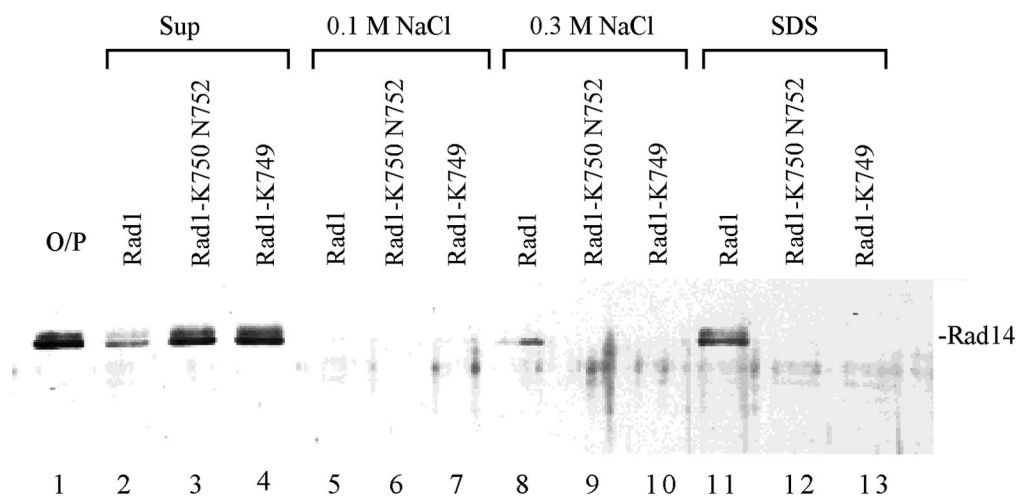

FIG. 4. Rad14 protein does not interact with the UV-sensitive Rad1 mutant proteins. Rad14 (lane1; O/P) was incubated with glutathione-Sepharose beads containing an equimolar amount of wild-type GST–Rad1-Rad10 protein complex. Rad14 present in the unbound supernatant fraction (lane 2), 0.1 M NaCl wash (lane 5), 0.3 M NaCl wash (lane 8), and in the SDS eluate (lane 11) was analyzed by immunoblotting with affinity-purified anti-Rad14 antibodies. The interaction of Rad14 with GST–Rad1-K750 N752-Rad10 (lanes 3, 6, 9, and 12) or GST–Rad1-K749-Rad10 (lanes 4, 7, 10, and 13) was determined as described above for the wild-type Rad1-Rad10 complex.
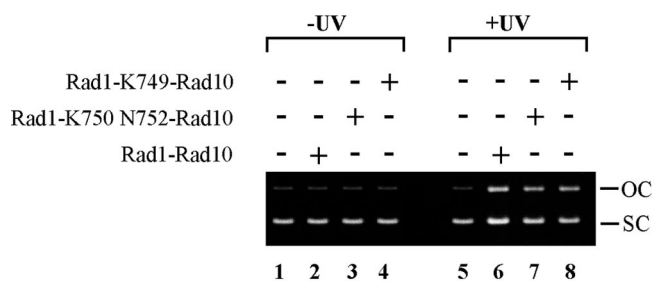
FIG. 5. UV-sensitive Rad1 mutant proteins support proficient incision of UV-damaged DNA in the in vitro system reconstituted from purified NER proteins. Replicative M13 mp18 DNA without (lanes 1 to 4) or with (lanes 5 to 8) UV treatment was incubated without (lanes 1 and 5) or with the NER factors consisting of purified TFIIH, Rad2, RPA, Rad14, or Rad4-Rad23 complex and, where indicated, either the wild-type Rad1-Rad10 complex (lanes 2 and 6), the Rad1-K750 N752-Rad10 complex (lanes 3 and 7), or the Rad1-K749-Rad10 complex (lanes 4 and 8). The reaction products were resolved on a 0.8% agarose gel and stained with ethidium bromide to reveal the proportion of supercoiled (SC) and open circular (OC) form DNA.

for the wild-type Rad1-Rad10 protein complex. As is shown in Fig. 5, both the mutant Rad1 proteins supported incision of UV-damaged DNA to almost the same degree as the wild-type Rad1 protein (compare lanes 7 and 8 to lane 6). Also, the mutant Rad1-Rad10 heterodimers did not show any evidence of aberrant nonspecific endonuclease activity on nondamaged DNA (compare lanes 3 and 4 to lane 2). Thus, in spite of the inability of the mutant Rad1-Rad10 nucleases to physically associate with Rad14, the endonuclease is proficiently targeted to the lesion sites on the plasmid DNA in this in vitro system.

DISCUSSION

Here we identify two mutations that specifically inactivate the NER function of Rad1 but have no effect on its recombination function. Both the Rad1 mutant proteins associate with Rad10 and form an endonuclease which displays the same pattern of incision activity as the wild-type protein on both the pseudo-Y and the bubble DNA substrates, which mimic the DNA intermediates that would be formed during the SSA type of recombination and during NER, respectively. The Rad1 mutant proteins, however, lack the ability to associate with Rad14; thereby, the ability of the Rad1-Rad10 nuclease to combine with Rad14 in NEF1 is severely jeopardized.

The fact that both the *rad1* mutations confer the same high degree of UV sensitivity to yeast cells as does the *rad1*Δ mutation indicates that in vivo these *rad1* mutations render yeast cells highly defective in the incision step of NER. Furthermore, the inability of the Rad1 mutant proteins to complex with Rad14 supports the inference that association with Rad14 is critical for endowing the Rad1-Rad10 nuclease with the ability to carry out its function in NER in vivo.

In spite of their inability to associate with Rad14, the Rad1 mutant proteins support the incision of UV-damaged plasmid DNA in the NER system reconstituted from purified proteins. However, since the incision reaction was performed under a single set of experimental conditions, we cannot rule out the possibility that under limiting conditions the mutant Rad1-

Rad10 nucleases become somewhat impaired in their incision proficiency. Still, we consider it highly unlikely that the high degree of UV sensitivity of the *rad1* mutants could have resulted from a marginal impairment in activity. How, then, could we explain the very different effects of these *rad1* mutations in the in vitro versus the in vivo situation? We suggest that since the in vitro assay conditions utilize high concentrations of NER proteins and the plasmid DNA bears a relatively high number of UV lesions, under these conditions, the Rad1-Rad10 nuclease is able to gain access to the lesion sites even when it is unable to associate with the Rad14 protein. Under the in vivo conditions, however, where relatively few DNA lesions are embedded in a vast excess of undamaged DNA and where the NER factors are present in very low abundance, for any effective targeting of the Rad1-Rad10 nuclease to the lesion sites to occur, it becomes paramount that the Rad1-Rad10 nuclease be in a complex with Rad14. We presume that in the absence of Rad14, the nuclease is unable to distinguish the damage sites from the vast excess of undamaged DNA and, hence, it becomes highly inept at accessing the lesion sites.

The ability of mutant Rad1 proteins to promote incision of UV-damaged DNA in the in vitro system suggests that the mutant Rad1-Rad10 enzyme complex retains the ability to assemble with the other NER proteins and to function in NER. Since, under the in vitro conditions, the Rad1-Rad10 nuclease is still targeted to the lesion sites, even when it cannot bind Rad14, we presume that interactions with the other NER proteins are sufficient for its targeting to UV lesions under the in vitro experimental conditions. These considerations lead us to suggest that the primary role of Rad14 as a component of NEF1 is to provide for an efficient targeting of the Rad1-Rad10 nuclease to the lesion sites in yeast cells. However, Rad14 is indispensable also for the in vitro incision reaction, as its omission from the reaction mix completely inhibits the incision of UV-damaged DNA (6). The fact that Rad14 is essential for the incision of UV-damaged DNA in the in vitro system (6), whereas its ability to interact with Rad1-Rad10 is not, points to yet another role for Rad14 in which it presumably modulates the assembly of NER proteins other than Rad1-Rad10.

In vivo, the Rad1-Rad10 nuclease participates in a variety of cellular processes that include NER (6), the SSA mode of recombination (5, 15), and the removal of 3′-blocked termini from DNA strand breaks that result from DNA damage induced by oxygen free radicals (9). Association with protein factors that enhance the capacity of Rad1-Rad10 nuclease to recognize the DNA substrates that are generated during these various cellular processes could be crucial for it to perform these different roles in a proficient manner. Thus, we expect the Rad1-Rad10 nuclease to be a part of different protein assemblies that promote its action in different cellular processes in which it participates. In that case, it should be possible to isolate mutations of *RAD1* that specifically inactivate its role in one of the cellular processes but have no effect upon the others and which confer defective interactions with a protein specifically involved in that particular cellular process. In further support of this idea, we have identified a mutation of *RAD1* that inactivates its recombination function but has no adverse effect on NER. We expect this *rad1* mutation to inactivate the ability of Rad1-Rad10 to associate with the recom-

bination protein(s) but not to affect its ability to combine with Rad14 or the other NER proteins.

Three different models, which cover the whole gamut of possibilities, have been proposed for the assembly of eukaryotic NER factors at the lesion sites. These range from a preassembled "repairosome," in which all the NER proteins are assembled into one large protein ensemble (31), to a model where the different NER proteins assemble as independent entities at the lesion site (25). Yet another model posits that the NER proteins exist in vivo in stable protein subassemblies which can be purified intact from cells (7, 24). Although the last model was originally proposed based upon studies of NER protein assemblies in yeast, the existence of stable protein complexes similar to those seen in yeast has also been documented for humans. Thus, similar to the tight association of Rad14 with the Rad1-Rad10 nuclease in NEF1 (7), of Rad4-Rad23 in NEF2 (6), and of Rad2 nuclease with TFIIH in NEF3 (12) in yeast, the XPA protein associates with the XPF-ERCC1 nuclease (22, 23), XPC complexes with the yeast Rad23 counterpart (17), and XPG copurifies with TFIIH (20) in humans. The very fact that the various eukaryotic NER proteins exist in vivo in tightly associated protein assemblies implies that NER would entail the sequential assembly of these various protein complexes at the lesion site rather than occurring via a preassembled "repairosome" or via the assembly of free NER proteins at the lesion site. And, our studies with the two *rad1* mutations that we report here provide strong genetic evidence that the ability of Rad1-Rad10 nuclease to associate in a complex with Rad14 is indispensable for the proficient targeting of this nuclease to the lesion sites in vivo.

ACKNOWLEDGMENT

REFERENCES

1. **Aravind, L., D. R. Walker, and E. V. Koonin.** 1999. Conserved domains in DNA repair proteins and evolution of repair systems. Nucleic Acids Res. **27:**1223–1242.
2. **Bailly, V., C. H. Sommers, P. Sung, L. Prakash, and S. Prakash.** 1992. Specific complex formation between proteins encoded by the yeast DNA repair and recombination genes *RAD1* and *RAD10*. Proc. Natl. Acad. Sci. USA **89:**8273–8277.
3. **Bardwell, A. J., L. Bardwell, A. E. Tomkinson, and E. C. Friedberg.** 1994. Specific cleavage of model recombination and repair intermediates by the yeast Rad1-Rad10 DNA endonuclease. Science **265:**2082–2085.
4. **Bardwell, L., A. J. Cooper, and E. C. Friedberg.** 1992. Stable and specific association between the yeast recombination and DNA repair proteins RAD1 and RAD10 in vitro. Mol. Cell. Biol. **12:**3041–3049.
5. **Fishman-Lobell, J., and J. E. Haber.** 1992. Removal of nonhomologous DNA ends in double-strand break recombination: the role of the yeast ultraviolet repair gene, *RAD1*. Science **258:**480–484.
6. **Guzder, S. N., Y. Habraken, P. Sung, L. Prakash, and S. Prakash.** 1995. Reconstitution of yeast nucleotide excision repair with purified Rad proteins, replication protein A, and transcription factor TFIIH. J. Biol. Chem. **270:**12973–12976.
7. **Guzder, S. N., P. Sung, L. Prakash, and S. Prakash.** 1996. Nucleotide excision repair in yeast is mediated by sequential assembly of repair factors and not by a pre-assembled repairosome. J. Biol. Chem. **271:**8903–8910.
8. **Guzder, S. N., P. Sung, L. Prakash, and S. Prakash.** 1997. Yeast Rad7-Rad16 complex specific for the nucleotide excision repair of the nontran-scribed DNA strand, is an ATP-dependent DNA damage sensor. J. Biol. Chem. **272:**21665–21668.
9. **Guzder, S. N., C. Torres-Ramos, R. E. Johnson, L. Haracska, L. Prakash, and S. Prakash.** 2004. Requirement of yeast Rad1-Rad10 nuclease for the removal of 3′-blocked termini from DNA strands breaks induced by reactive oxygen species. Genes Dev. **18:**2283–2291.
10. **Haber, J. E.** 1992. Exploring the pathways of homologous recombination. Curr. Opin. Cell Biol. **4:**401–412.
11. **Habraken, Y., P. Sung, L. Prakash, and S. Prakash.** 1993. Yeast excision repair gene *RAD2* encodes a single-stranded DNA endonuclease. Nature **366:**365–368.
12. **Habraken, Y., P. Sung, S. Prakash, and L. Prakash.** 1996. Transcription factor TFIIH and DNA endonuclease Rad2 constitute yeast nucleotide excision repair factor 3: implications for nucleotide excision repair and Cockayne syndrome. Proc. Natl. Acad. Sci. USA **93:**10718–10722.
13. **Haracska, L., R. E. Johnson, I. Unk, B. Phillips, J. Hurwitz, L. Prakash, and S. Prakash.** 2001. Physical and functional interactions of human DNA polymerase η with PCNA. Mol. Cell. Biol. **21:**7199–7206.
14. **Hartwell, L. H., and D. Smith.** 1985. Altered fidelity of mitotic chromosome transmission in cell cycle mutants of *S. cerevisiae*. Genetics **110:**381–395.
15. **Ivanov, E. L., and J. E. Haber.** 1995. *RAD1* and *RAD10*, but not other excision repair genes, are required for double-strand break-induced recombination in *Saccharomyces cerevisiae*. Mol. Cell. Biol. **15:**2245–2251.
16. **Johnston, L. H., and K. A. Nasmyth.** 1978. *Saccharomyces cerevisiae* cell cycle mutant *cdc9* is defective in DNA ligase. Nature **274:**891–893.
17. **Masutani, C., K. Sugasawa, J. Yanagisawa, T. Sonoyama, M. Ui, T. Enomoto, K. Takio, K. Tanaka, P. J. van der Spek, D. Bootsma, J. H. J. Hoeijmakers, and F. Hanaoka.** 1994. Purification and cloning of a nucleotide excision repair complex involving the xeroderma pigmentosum group C protein and a human homologue of yeast RAD23. EMBO J. **13:**1831–1843.
18. **Montelone, B. A., S. Prakash, and L. Prakash.** 1981. Spontaneous mitotic recombination in *mms8-1*, an allele of the *CDC9* gene of *Saccharomyces cerevisiae*. J. Bacteriol. **147:**517–525.
19. **Mu, D., D. S. Hsu, and A. Sancar.** 1996. Reaction mechanism of human DNA repair excision nuclease. J. Biol. Chem. **271:**8285–8294.
20. **Mu, D., C.-H. Park, T. Matsunaga, D. S. Hsu, J. T. Reardon, and A. Sancar.** 1995. Reconstitution of human DNA repair excision nuclease in a highly defined system. J. Biol. Chem. **270:**2415–2418.
21. **Newman, M., J. Murray-Rust, J. Lally, J. Rudolf, A. Fadden, P. P. Knowles, M. F. White, and N. Q. McDonald.** 2005. Structure of an XPF endonuclease with and without DNA suggests a model for substrate recognition. EMBO J. **24:**895–905.
22. **Park, C.-H., T. Bessho, T. Matsunaga, and A. Sancar.** 1995. Purification and characterization of the XPF-ERCC1 complex of human DNA repair excision nuclease. J. Biol. Chem. **270:**22657–22660.
23. **Park, C.-H., and A. Sancar.** 1994. Formation of a ternary complex by human XPA, ERCC1, and ERCC4(XPF) excision repair proteins. Proc. Natl. Acad. Sci. USA **91:**5017–5021.
24. **Prakash, S., and L. Prakash.** 2000. Nucleotide excision repair in yeast. Mutat. Res. **451:**13–24.
25. **Rademakers, S., M. Volker, D. Hoogstraten, A. L. Nigg, M. J. Mone, A. A. van Zeeland, J. H. J. Hoeijmakers, A. B. Houtsmuller, and W. Vermeulen.** 2003. Xeroderma pigmentosum group A protein loads as a separate factor onto DNA lesions. Mol. Cell. Biol. **23:**5755–5767.
26. **Reardon, J. T., and A. Sancar.** 2002. Molecular anatomy of the human excision nuclease assembled at sites of DNA damage. Mol. Cell. Biol. **22:**5938–5945.
27. **Reardon, J. T., and A. Sancar.** 2003. Recognition and repair of the cyclobutane thymine dimer, a major cause of skin cancers, by the human excision nuclease. Genes Dev. **17:**2539–2551.
28. **Schiestl, R. H., and S. Prakash.** 1988. *RAD1*, an excision repair gene of *Saccharomyces cerevisiae*, is also involved in recombination. Mol. Cell. Biol. **8:**3619–3626.
29. **Schiestl, R. H., and S. Prakash.** 1990. *RAD10*, an excision repair gene of *Saccharomyces cerevisiae*, is involved in the *RAD1* pathway of mitotic recombination. Mol. Cell. Biol. **10:**2485–2491.
30. **Sung, P., P. Reynolds, L. Prakash, and S. Prakash.** 1993. Purification and characterization of the *Saccharomyces cerevisiae* RAD1/RAD10 endonuclease. J. Biol. Chem. **268:**26391–26399.
31. **Svejstrup, J. Q., Z. Wang, W. J. Feaver, X. Wu, D. A. Bushnell, T. F. Donahue, E. C. Friedberg, and R. D. Kornberg.** 1995. Different forms of TFIIH for transcription and DNA repair: holo-TFIIH and a nucleotide excision repairosome. Cell **80:**21–28.